NMR IN BIOMEDICINE
NMR Biomed. 2002;**15**:89–98
Published online in Wiley InterScience (www.interscience.wiley.com). DOI: 10.1002/nbm.754

Evaluation of the anti-vascular effects of combretastatin in rodent tumours by dynamic contrast enhanced MRI

Ross J. Maxwell,[1]* John Wilson,[1] Vivien E. Prise,[1] Borivoj Vojnovic,[1] Gordon J. Rustin,[2] Martin A. Lodge[3] and Gillian M. Tozer[1]

[1]Gray Cancer Institute, Mount Vernon Hospital, Northwood, Middlesex, UK
[2]Cancer Treatment Centre, Mount Vernon Hospital, Northwood, Middlesex, UK
[3]Paul Strickland Scanner Centre, Mount Vernon Hospital, Northwood, Middlesex, UK

Received 6 February 2001; Revised 1 October 2001; Accepted 5 October 2001

ABSTRACT: The anti-vascular effects of the tubulin binding agent, disodium combretastatin A-4 3-*O*-phosphate (CA-4-P), have been investigated in the rat P22 carcinosarcoma by measurements of radiolabelled iodoantipyrine uptake and dynamic contrast-enhanced MRI. The iodoantipyrine estimates of absolute tumour blood flow showed a reduction from 0.35 to 0.04 ml g^{-1} min^{-1} 6 h after 10 mg kg^{-1} CA-4-P and to <0.01 ml g^{-1} min^{-1} after 100 mg kg^{-1}. Tumour blood flow recovered to control values 24 h after 10 mg kg^{-1} CA-4-P, but there was no recovery by 24 h after the higher dose. Dynamic contrast-enhanced MR images were obtained at 4.7 T, following injection of 0.1 mmol kg^{-1} Gd-DTPA and analysed assuming a model arterial input function. A parameter, K^{trans}, which is related to blood flow rate and permeability of the tumour vasculature to Gd-DTPA, was calculated from the uptake data. K^{trans} showed a reduction from 0.34 to 0.11 min^{-1} 6 h after 10 mg kg^{-1} CA-4-P and to 0.07 min^{-1} after 100 mg kg^{-1}. Although the magnitude of changes in K^{trans} was smaller than that in tumour blood flow, the time course and dose-dependency patterns were very similar. The apparent extravascular extracellular volume fraction, ν_e, showed a four-fold reduction 6 h after 100 mg kg^{-1} CA-4-P, possibly associated with vascular shutdown within large regions of the tumour. These results suggest that K^{trans} values for Gd-DTPA uptake into tumours could be a useful non-invasive indicator of blood flow changes induced by anti-vascular agents such as combretastatin. Copyright © 2002 John Wiley & Sons, Ltd.

INTRODUCTION

Anti-vascular and anti-angiogenic drugs are currently of great interest in the treatment of cancer.[1,2] Use of these drugs is aimed at inducing secondary tumour cell death via selectively destroying or inhibiting the formation of tumour blood vessels, respectively. Disodium combretastatin A-4 3-*O*-phosphate (CA-4-P) is a tubulin-binding agent which has been shown to depolymerize the tubulin cytoskeleton of vascular endothelial cells *in vitro* and to selectively shut down tumour blood flow in animal models *in vivo*.[3–5] For clinical trials and the further development of anti-vascular agents, methods for clinically evaluating the vascular response of both tumour and normal tissues to treatment are urgently required.

Dynamic contrast enhanced MRI (DCE-MRI) of the tissue uptake of gadolinium diethylenetriamine-pentaacetic acid (Gd-DTPA) has been used in phase 1 trials of CA-4-P to evaluate the extent and time course of its anti-vascular effect in human tumours.[6] However, DCE-MRI with Gd-DTPA does not provide an unambiguous measurement of tumour blood flow since the kinetics of the uptake of this contrast agent into tissues is also sensitive to the vascular permeability–surface area product.[7] This particularly complicates the interpretation of CA-4-P effects since drug-induced depolymerization of the cytoskeleton of endothelial cells is expected to increase vascular permeability (to macromolecules, at least) as well as reducing blood flow.

The present study aimed to evaluate DCE-MRI with Gd-DTPA, as a means of monitoring tumour blood flow changes after CA-4-P treatment, using a rat tumour model. The time-course of parameter changes obtained by DCE-MRI, following CA-4-P treatment, was compared with the time-course of changes in absolute tumour blood flow, measured by the uptake of radiolabelled iodoantipyrine (a freely diffusible tracer). The DCE-MRI protocol used for the phase 1 clinical trials of CA-4-P at Mount Vernon Hospital, was implemented for the animal studies with two modifications. Firstly, a higher spatial resolution was obtained and secondly, pre-contrast T_1 mapping was implemented. Unsupervised cluster analy-

**Correspondence to:* R. J. Maxwell, Gray Cancer Institute, PO Box 100, Mount Vernon Hospital, Northwood, Middlesex HA6 2JR, UK. Email: maxwell@gci.ac.uk

Abbreviations used: CA-4-P, disodium combretastatin A-4 3-*O*-phosphate; DCE-MRI, dynamic contrast enhanced MRI; Gd-DTPA, gadolinium diethylenetriamine-pentaacetic acid; IAP, iodoantipyrine; IR, inversion recovery; NN, neural network.

sis[8] was used to identify pixels with similar Gd-DTPA kinetics, which were then averaged before mathematical fitting of T_1 and DCE-MRI data.

METHODS

Tumour model

Male rats bearing subcutaneously implanted P22 carcinosarcomas[9] on the flank were studied when the tumour diameter was approximately 16 mm. Animals were treated with CA-4-P in saline (10 or 100 mg kg^{-1}, provided by OxiGene Inc.) by intraperitoneal injection at approximately 3 ml kg^{-1}. A few drops of 5% sodium carbonate were added for complete dissolution of CA-4-P at the high dose. Control rats received saline alone. MRI examination was carried out at 1, 6 or 24 h after CA-4-P. Radiotracer measurements of absolute tumour blood flow were made at 1, 6, 12 or 24 h after CA-4-P. Rats were anaesthetized for tail vessel cannulation, MRI procedures and radiotracer procedures using intraperitoneal injection of fentanyl citrate (0.32 mg kg^{-1}) and fluanisone (10 mg kg^{-1}; Hypnorm, Janssen Animal Health) and midazolam (5 mg kg^{-1}; Hypnovel, Roche). Top-up anaesthesia was used as required. Rat body temperature was maintained in the magnet using a recirculating warm water system and, during radiotracer studies, using a thermostatically controlled heating pad. Separate groups of animals were used for the different dose groups and for MRI and radiotracer studies.

Radiotracer experiments

Absolute tumour blood flow was measured using the uptake, over a short infusion time, of the inert, readily diffusible compound, iodoantipyrine radiolabelled with ^{125}I (^{125}I-IAP, Institute of Cancer Research). This method has been published previously.[9] Briefly, animals were heparinized within minutes of blood flow measurement to avoid the interaction of heparin with any pro-coagulant effects of CA-4-P. At the assay time, approximately 0.3 MBq (8 μCi) of ^{125}I-IAP were infused into a cannulated tail vein for 30 s, at a rate of 1.6 ml min^{-1}. During the 30 s, free-flowing blood from a cannulated artery was collected at 1 s intervals into pre-weighed vials. At the end of 30 s, the rat was killed rapidly by i.v. injection of sodium pentobarbitone (200 mg ml^{-1}, Euthatal, Rhone Merieux, Harlow, Essex, UK) and the tumour rapidly excised. Radioactivity in the tumour and blood samples was counted in a Wallac Autogamma well-counter.

Calculation of tumour blood flow rate was based on the Kety[10] model for tissue uptake of an inert, readily diffusible tracer:

$$C_t(t) = k_1 \cdot C_a(t) \otimes \exp(-k_2 \cdot t) \qquad (1)$$

where $C_t(t)$ is concentration of the tracer in the tumour as a function of time, t, in counts per minute per g tissue; k_1 is tumour blood flow rate in ml blood per g tissue per minute; $C_a(t)$ is the concentration of the tracer in arterial blood entering the tumour as a function of t, in counts per minute per ml whole blood (arterial input function), $\otimes$ denotes the convolution integral and $k_2 = k_1/V_d$ where V_d is the apparent volume of distribution of the tracer in the tumour tissue (in Kety's formulation, the partition coefficient, λ, is used instead of V_d). A value of 0.8 was used for V_d.[11] The arterial counts were corrected for timing differences between blood collection and blood in the arterial circulation and dispersion or smearing of the blood, as it travels down the plastic cannula, using an exponential model.[12] The expected value of $C_t(t)$ at 30 s (the end of the infusion time) was calculated over a range of blood flow rates, using eqn (1);, to give a look-up table for each individual tumour, from which the corresponding k_1 (tumour blood flow rate) was obtained.[9,12]

MRI

Animals were placed in the 4.7 T, 30 cm diameter horizontal bore magnet of a Varian Inova MR spectroscopy/imaging system (Varian, Palo Alto, CA, USA). A 3.0 cm diameter, two-turn surface coil was placed around the tumour as a transmitter/receiver.

Pre-contrast T_1 values were determined from an inversion recovery (IR) sequence. The sequence consisted of a 180° sinc pulse followed by a variable interval, *TI* (150, 450, 1300 and 2900 ms), then a spin echo period (*TE* = 10 ms) with 1 ms gaussian pulses. Other parameters were: *TR* = 3000 ms; 2 mm slice thickness; field of view 30 × 30 mm; 256 × 64 data points. Therefore a set of four IR images were obtained for each tumour.

A set of 30 dynamic-contrast enhanced (DCE) gradient echo images were obtained with time resolution of 11.8 s per image. Three images were obtained before and the remainder after administration of contrast agent. The contrast agent, Gd-DTPA (Magnevist, Schering), was administered at a dose of 0.1 mmol kg^{-1} in a volume of 1.0 ml kg^{-1} over 5 s via an infusion pump connected to a cannulated tail vein. MRI parameters used were: *TR*, 80 ms; *TE*, 10 ms; flip angle, 30°; 2 mm slice thickness; field of view 30 × 30 mm; and 256 × 148 data points (giving 0.12 × 0.20 mm in-plane resolution).

Data processing

Images were processed using Matlab version 5 (The Mathworks, Natick, MA, USA). Initial processing of IR and DCE images involved zero-filling and two-dimensional Fourier transformation to give 256 × 256 data points per image. A region of interest was drawn around the tumour from the IR image with *TI* = 2900 ms,

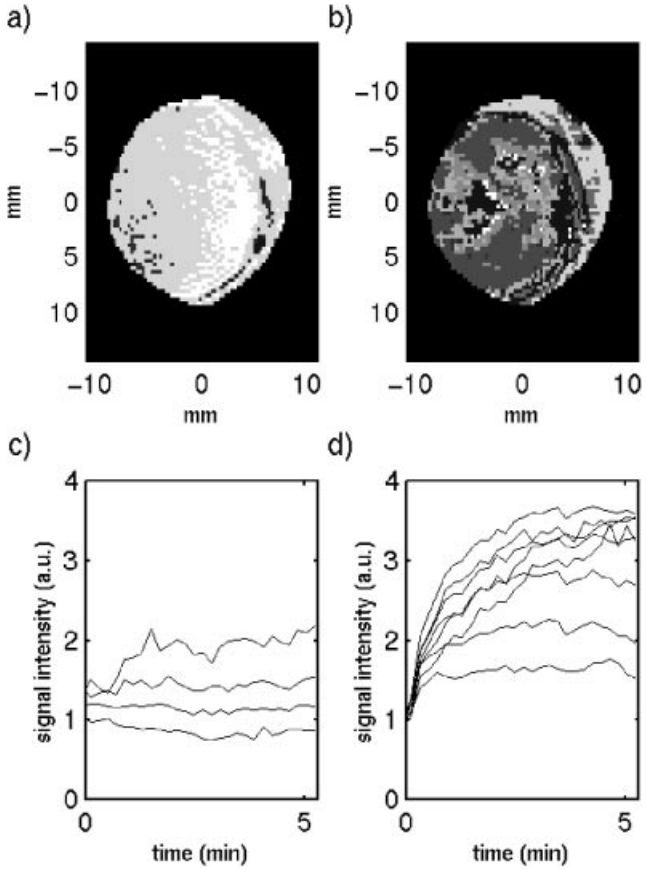

Figure 1. Neural network image segmentation based on (a) saline injection and (b) Gd-DTPA injection. The different grey levels indicate pixels segmented into different clusters. Mean image intensity profiles for segmented regions (c) for saline injection and (d) for Gd-DTPA injection

typically corresponding to 10000–20000 pixels. The DCE-MRI data for each of these pixels was re-organized into 28 point vectors: a background value (mean of second and third images) followed by post-contrast values from each of the subsequent 27 images.

Neural network (NN) cluster analysis was used to segment the images into up to eight classes having similar kinetics of contrast-induced signal intensity changes.[8] This process starts with eight random 28-point vectors. A vector from one pixel is then presented to the competitive NN. The most similar of the NN vectors is chosen and is reinforced, becoming yet more similar to the data vector. This process is repeated many times (3000 pixel vectors are randomly picked for presentation to the NN). At the end of the unsupervised NN learning, all of the pixel vectors are evaluated for their similarity to the eight NN vectors, some or all of which are now representative of the DCE-MRI data, i.e. each pixel is allocated to one of the NN vectors and the image is segmented into up to eight classes. This method is described in more detail elsewhere.[8] Figure 1 illustrates the segmentation results for a tumour following injection of saline [Fig. 1(a) and (c)] or 0.1 mmol kg^{-1} Gd-DTPA 15 min later [Fig. 1(b) and (d)]. In the case of segmentation based on Gd-DTPA contrast-enhanced time series, up to eight classes were identified, the mean kinetics for each class of pixels being shown in Fig. 1(d). By comparison, segmentation based on a control time-series was (i) completely different from the segmentation with Gd-DTPA; (ii) generally more uniform spatially [Fig. 1(a)]; and (iii) generally resulted in fewer classes of pixels [Fig. 1(c)]. It should be noted that as this approach is unsupervised, the segmentation is not necessarily 'optimum' in any particular sense, it is merely one way of selecting groups of pixels with similar patterns of contrast enhancement.

T_1 values were calculated for each cluster using the mean IR data for the pixels of that cluster using a three-parameter non-linear least squares fitting procedure. This estimate of T_1 was used to convert image intensity into Gd-DTPA concentration [$C_t(t)$] on a pixel-by-pixel basis. The mean contrast agent kinetics was determined for each cluster and fit to:

$$C_t(t) = K^{trans} \cdot C_a(t) \otimes \exp(-k_{ep} \cdot t) \qquad (2)$$

Equation (2), describing Gd-DTPA kinetics is identical to eqn (1), describing IAP kinetics, except that the notation proposed[13] for MR studies is used in eqn (2). k_1 or K^{trans} is equivalent to $F{\cdot}E$ where F is the blood flow rate and E is the extraction fraction. For IAP, E is assumed to be 1.0 and k_1 reduces to F, the blood flow rate. For Gd-DTPA, $E = 1 - \exp(-P \cdot S/F)$, with P being vascular permeability to the tracer and S being the vascular surface area.[13] Compared to the time-resolution used for dynamic imaging (11.8 s), there was very little variability in 'lag period' between injection of contrast agent and appearance in the tumour, and no corrections were used for the fitting.

Therefore in eqn (2), K^{trans} is the volume transfer constant (min^{-1}).[13] k_2 is replaced by k_{ep}, the rate constant for backflux of Gd-DTPA from the extravascular extracellular space, ν_e, to the plasma (min^{-1}), $k_{ep} = F{\cdot}E/v_e$.[13] $C_a(t)$ is the assumed arterial concentration of Gd-DTPA (mM in plasma) based on the parameters described for rats where plasma (and urine) data were modelled as a three-exponential equation:[14]

$$C_a(t) = A1 \cdot \exp(-\alpha_1 \cdot t) + A2 \cdot \exp(-\alpha_2 \cdot t) + A3 \cdot \exp(-\alpha_3 \cdot t) \qquad (3)$$

Using the rate constants given[14] for a three-compartment open model[15] gives $A1 = 0.8259$ mM, $A2 = 0.2230$ mM, $A3 = 0.1565$ mM, $\alpha_1 = 1.220\ min^{-1}$, $\alpha_2 = 0.156\ min^{-1}$ and $\alpha_3 = 0.017\ min^{-1}$ for a dose of 0.1 mmol kg^{-1}. Parametric maps of K^{trans}, k_{ep} and ν_e ($v_e = K^{trans}/k_{ep}$), were calculated for each tumour.

Gd-DTPA kinetic parameters were also calculated (i) from Gd-DTPA concentration averaged over the whole tumour and (ii) from Gd-DTPA concentration on a pixel-by-pixel basis. The following criteria were used for the

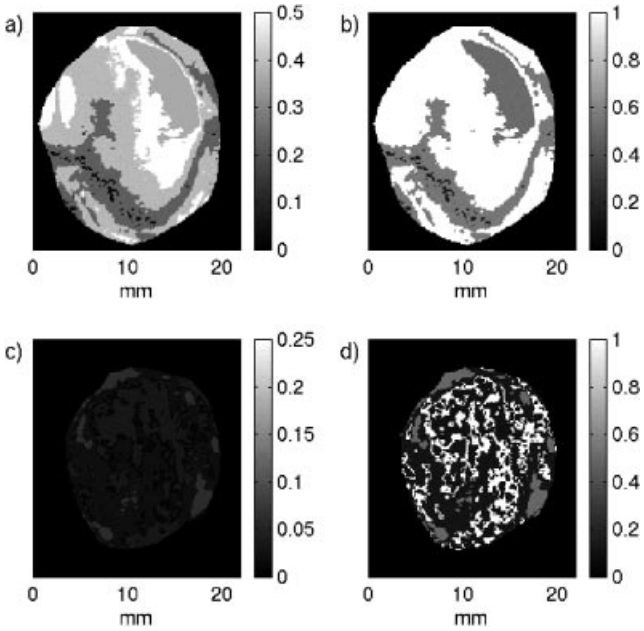

Figure 2. (a) K^{trans} map and (b) ν_e map for control tumour; (c) K^{trans} map and (d) ν_e map for tumour 6 h after CA-4-P 100 mg kg^{-1}

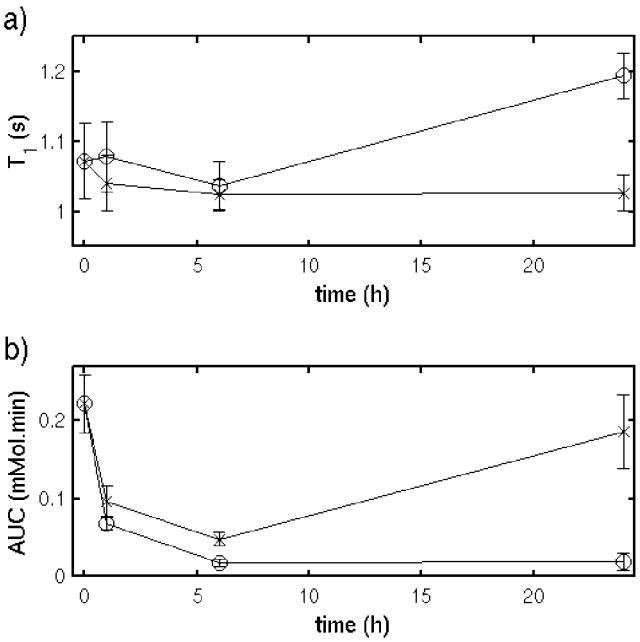

Figure 3. Effect of CA-4-P 10 mg kg^{-1} (×) and 100 mg kg^{-1} (○) on tumour parameters: (a) ^{1}H T_1; (b) area under [Gd-DTPA] curve (AUC) from 0 to 94 s

rejection only of pixels considered to be very extreme outliers (pixels accepted where $0.00001 < K^{trans} < 100$ min^{-1} and $0.00001 < k_{ep} < 100$ min^{-1} and $v_e < 3$); pixels with parameters outside of these ranges were excluded from further analysis except for those with low K^{trans} values, which were included but reset to the minimum value (0.00001 min^{-1}). For parametric maps calculated both on a pixel-by-pixel basis and using segmented data, the distance of each pixel from the tumour edge was also determined such that kinetic parameters could be summarized in three categories according to distance from tumour edge: rim (0–2.0 mm from edge); intermediate (2.0–5.0 mm) and centre (>5.0 mm).

In addition, area-under-the-curve (AUC) for Gd-DTPA concentration was calculated for each tumour by summing the vales from the first eight post-contrast images (0–94 s).

Statistics

All data were tested for normality of distribution and equal variances between groups using a Shapiro–Wilk *W*-test and an O'Brien's *F*-test, respectively. In the majority of cases, these conditions were fulfilled and differences between treated groups and controls were tested for significance using a standard ANOVA followed by the Dunnett's test. Student's *t*-test (corrected for multiple comparisons) was used for testing the significance of differences between different dose groups. The Wilcoxon rank-sum test for non-parametric data was used for groups that failed the test for normality and Student's *t*-test for unequal variances was used where appropriate. A paired *t*-test was used for comparing data from different tumour regions.

RESULTS

Figure 2 shows a comparison of K^{trans} and ν_e maps calculated using the image segmentation protocol for a control tumour [Fig. 2(a) and 2(b)] and a tumour 6 h after treatment with CA-4-P 100 mg kg^{-1} [Fig. 2(c) and 2(d)]. The treated tumour showed much lower K^{trans} and ν_e values except for a small number of pixels.

The effects of combretastatin on T_1 and AUC (area under the Gd-DTPA concentration–time curve from 0–94 s) are summarized in Fig. 3. There was no significant change in mean tumour T_1 relaxation time [Fig. 3(a)] following combretastatin treatment except, possibly, for the 100 mg kg^{-1} at 24 h group ($P < 0.05$ for the difference between 10 and 100 mg kg^{-1} at 24 h but the difference between 100 mg kg^{-1} at 24 h and control is not significant). The effects of combretastatin on the model parameters K^{trans}, k_{ep} and ν_e calculated using the image segmentation protocol[8] are shown in Fig. 4. The parameter K^{trans} showed the most marked change [Fig. 3(a)] with a maximal effect 6 hours after combretastatin treatment (three-fold reduction at 10 mg kg^{-1}; five-fold reduction at 100 mg kg^{-1}). K^{trans} recovered to control values 24 h after the low dose but not after the high dose treatment. k_{ep} did not show any significant changes but

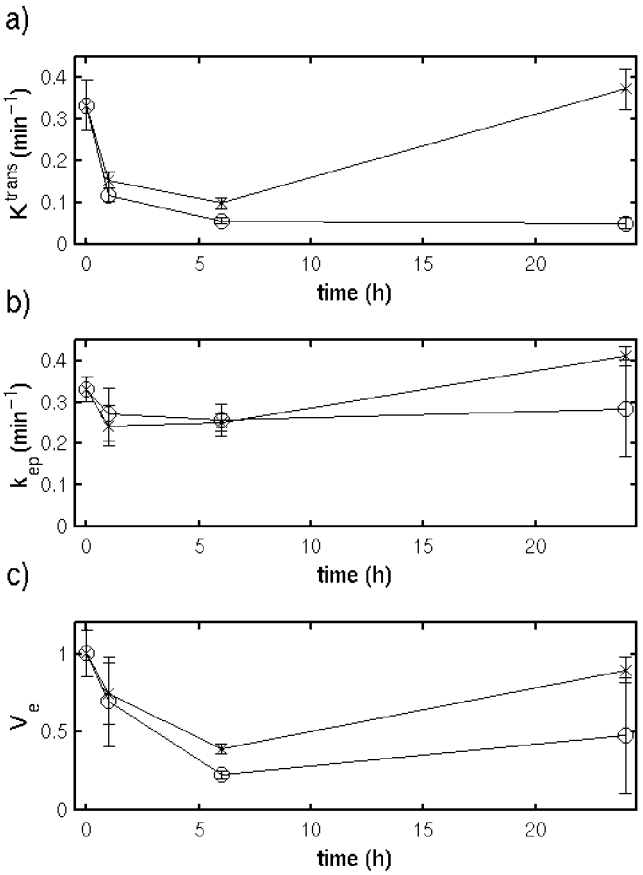

Figure 4. Effect of CA-4-P 10 mg kg^{-1} (×) and 100 mg kg^{-1} (○) on model parameters: (a) K^{trans}; (b) k_{ep}; (c) ν_e

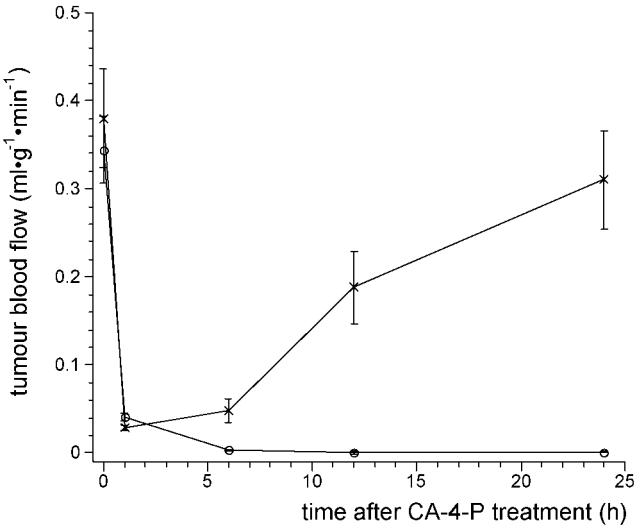

Figure 5. Effect of CA-4-P 10 mg kg^{-1} (×) and 100 mg kg^{-1} (○) on tumour blood perfusion determined by IAP uptake

estimation of this parameter was more difficult when tumour Gd-DTPA uptake was low. The largest apparent change in k_{ep} occurred at 1 h after treatment with the lower dose, but even this was not statistically significant ($P = 0.07$). ν_e was also found to decrease after treatment as would be expected from the fall in K^{trans} without any significant change in k_{ep}. The relative changes in AUC [Fig. 3(b)] were similar to those in K^{trans}.

Very similar results to those described above were obtained when the parameters were calculated from data averaged over the entire tumour region (data not shown). However, somewhat different results were obtained when the uptake data were analysed on a pixel-by-pixel basis. The reductions in K^{trans} and ν_e after CA-4-P treatment were more marked according to this analysis. A substantial increase in k_{ep} was apparent, 6 h after a dose of 100 mg kg^{-1} in the intermediate and central regions of the tumour (data not shown). However, a relatively large proportion of pixel values (15–30%) was rejected, mostly because of unacceptably low k_{ep} values or high ν_e values. This casts some doubt on the robustness of the pixel-by-pixel analysis.

Figure 5 shows the effect of CA-4-P on tumour blood flow rate using the uptake of ^{125}I-IAP. The pattern of change is very similar to that shown in Figs 3(b) and 4(a) for the effect of CA-4-P on the MR parameters, AUC and K^{trans}, respectively. However, the relative reduction in blood flow rate at 1 and 6 h is somewhat larger, with an 8-fold reduction at 6 h following 10 mg kg^{-1} and a collapse to practically zero at 6 h following 100 mg kg^{-1}. The data in Fig. 5 were found to be relatively insensitive to the value used for V_d. For instance, blood flow rate only increased by $9.8 \pm 2.8\%$ (mean $\pm$ 1 SEM) if a value of 0.1, instead of 0.8, was used in the calculations for the 10 mg kg^{-1} dose group at 6 h.

Comparison of Figs 4(a) and 5 suggests a correlation between tumour blood flow, F, determined by IAP uptake for each treatment group and mean K^{trans} values for the same treatments (determined from parallel groups of animals). In addition to a strong correlation between these parameters ($r = 0.98$, $p < 0.001$), the values were also found to be numerically similar ($F = -0.88 + 1.13 \times K^{trans}$).

Analysis of kinetic parameters using the segmented data was also performed according to the distance from the tumour edge (rim, $<$ 2.0 mm from tumour edge; intermediate, 2.0–5.0 mm from tumour edge; and centre, $>$5.0 mm from tumour edge). Figure 6 summarizes these results for (a) K^{trans} and (b) ν_e for Gd-DTPA in the control and 10 mg kg^{-1} CA-4-P treatment groups. Figure 6(c) shows similar plots of AUC (0–94 s) calculated from pixel-by-pixel analysis. In the case of untreated tumours, no significant spatial differences were identified for K^{trans}, k_{ep}, ν_e or AUC. In addition, the reduction in K^{trans} appeared to occur uniformly across the tumours (i.e. there were no differences between the rim, intermediate and central tumour regions for tumours treated with CA-4-P). The reduction in ν_e at 6 and 24 h after 10 or 100 mg kg^{-1} CA-4-P seemed to be slightly greater at the tumour centre than at the rim [Fig. 6(b)], but this difference was not statistically significant. The pixel-by-pixel analysis

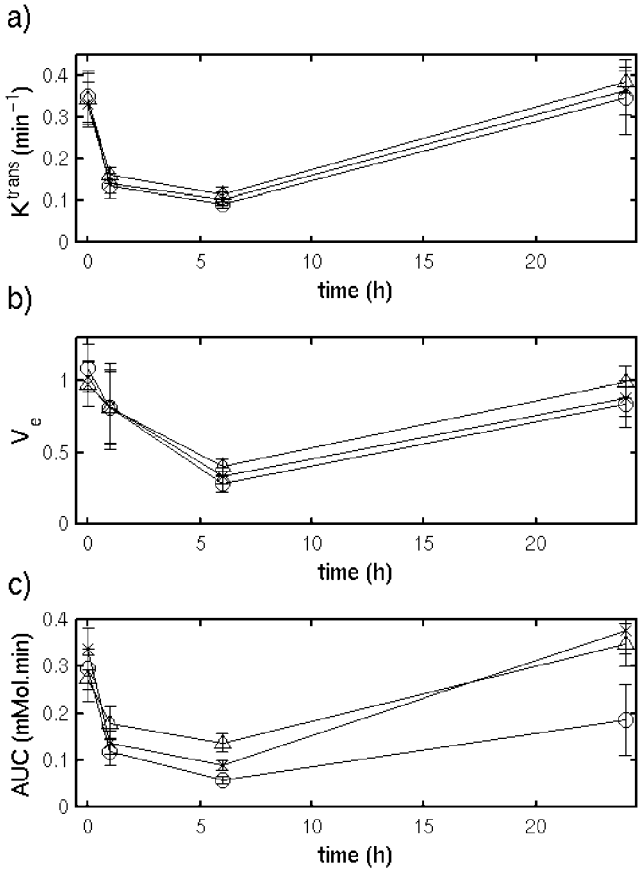

Figure 6. Effect of CA-4-P 10 mg kg^{-1} on (a) K^{trans}, (b) ν_e and (c) AUC (0–94 s) according to position in the tumour: (Δ) rim (0–2.0 mm from edge); (×) intermediate (2.0–5.0 mm from edge); (○) centre (>5.0 mm from edge)

suggested a higher k_{ep} and lower ν_e at the rim than in intermediate or central parts of untreated tumours. Reductions in K^{trans} and ν_e were generally greater towards the tumour centre (data not shown). CA-4-P resulted in a reduction in k_{ep} in the tumour rim only, whereas an increase in k_{ep} was apparent at 6 h in intermediate and central regions (after 10 or 100 mg kg^{-1}). However, a substantial proportion of pixels (15–30%) was excluded from the pixel-by-pixel estimation of model parameters because the calculated parameters were outside of the realistic range (usually due to unacceptably low k_{ep} values or high ν_e values). Pixel-by-pixel analysis of AUC values was more robust than for K^{trans}, k_{ep} or ν_e as model fitting was not required. There was a suggestion of a more marked effect in the tumour centre [Fig. 6(c)], but the only statistically significant difference indicated that the AUC in the rim was higher than that in the centre at 6 h after 10 mg kg^{-1} CA-4-P ($p < 0.05$).

DISCUSSION

^{31}P MRS and several MRI approaches have previously been used to study the effects of CA-4-P on subcutaneous sarcoma F tumours in mice.[17] A fall in energetic status (2-fold increase in P_i/NTP) and in tumour pH were observed 2.5 h after treatment with 100 mg kg^{-1}. The rate of uptake of Gd-DTPA into the tumour centre was decreased 2.5-fold with a smaller effect at the tumour periphery. Changes in T_2-weighted images (i.e. slight increases in the area of low signal intensity regions), 3 h after treatment, were ascribed to haemorrhage, consistent with histological changes. MRS and MRI techniques were also used to study the effects of CA-4-P (100 mg kg^{-1}) on C3H mammary tumours implanted on the mouse foot.[18] The ^{31}P MRS results were similar to those in sarcoma F,[17] although an additional measurement at 24 h after treatment showed full recovery of NTP/P_i. Single-voxel ^{1}H MRS measurements of lactate did not show a consistent increase, possibly due to lipid contamination and/or a reduction in glucose supply associated with blood flow reduction. No increases in low signal intensity regions of T_2-weighted MR images were detected within 3 h of CA-4-P treatment. In the case of the C3H mammary tumour, histology showed no significant increase in tumour necrosis 3 h after treatment, although an increase in necrosis from 2 to 16% was observed at 24 h. The extent of haemorrhagic necrosis may vary between anti-vascular therapies and tumour types but these data imply that haemorrhage is not a prerequisite for CA-4-P-induced tumour blood flow reduction.

Comparison of IAP and Gd-DTPA measurements

Although the reduction in K^{trans} following CA-4-P was smaller than that in tumour blood flow rate determined by IAP uptake, the estimated values of K^{trans} and blood flow rate in parallel groups of untreated and CA-4-P treated rats show a relatively good correspondence. How do we expect these parameters to be related? In general, K^{trans} and k_{ep} cannot readily be related to blood flow rate (F) because of the influence of $P{\cdot}S$ and when $P{\cdot}S \ll F$, the effect of $P{\cdot}S$ is dominant. For a freely diffusible tracer ($P{\cdot}S \gg F$), $E = 1$. We note that if $P{\cdot}S$ has an effect on Gd-DTPA kinetics in untreated tumours (where F is relatively high), treatment with CA-4-P (which reduces F and may increase P) could cause a shift to the situation where F is the dominant influence. In addition, it should be noted that a correction for haematocrit should be applied in the case of an extracellular tracer such as Gd-DTPA since it is present in plasma and not in blood cells[13] and the plasma concentration has been used for the arterial input function. However, choice of an appropriate correction factor is complicated since the haematocrit of tumour-bearing rats can be substantially lower than that of normal rats and the haematocrit in tissue and tumour blood vessels may be lower than in large vessels.[11] No correction for haematocrit has been applied in this study,

therefore if Gd-DTPA kinetics are flow-limited, K^{trans} will be a measure of plasma flow rate rather than that of whole blood.

In addition, the method of calculating F using IAP measurements is different from the analysis of Gd-DTPA measurements. In the case of IAP, a fixed value of V_d is assumed and used to obtain look-up tables relating the concentration of IAP in tissue at 30 s to the measured arterial concentration time course. Although IAP is considered to be a freely diffusible tracer, the presence of macroscopic regions of tumour ischaemia certainly lead to a reduction in V_d and/or diffusion-limited kinetics.[12] It is clear that since the analogous parameter, ν_e, in the Gd-DTPA analysis shows significant changes in response to CA-4-P treatment, the assumption of a fixed value for V_d is, strictly, incorrect. However, over the short infusion time of IAP used in these experiments, the calculations are relatively insensitive to changes in V_d and changing the value used for V_d from 0.8 to 0.1 made very little difference to the calculated tumour blood flow rate following CA-4-P treatment (see Results section). Both ν_e (in the case of Gd-DTPA) and V_d (in the case of IAP) are analagous parameters that can be considered to be the 'volume of distribution' for their respective tracers in tissue. Volume of distribution is defined as the equilibrium ratio of the amount of tracer in a unit mass of tissue to the concentration of tracer in blood. It can be thought of as the fractional volume of tissue space that a tracer would occupy with the same concentration as in blood. Although it is not clear whether Gd-DTPA has the same concentration in tissue as it does in blood, ν_e has been interpreted as the volume of extravascular extracellular space.[14] If this interpretation is correct, ν_e would be expected to lie in the range 0.0–1.0 whereas, in general, volumes of distribution are not limited in this way, e.g. Wedeking *et al.*[14] report the V_d of Gd-DTPA in the plasma compartment as being 340% of the expected plasma volume. We note that the ν_e values estimated for untreated P22 tumours in this study are close to 1.0 and that this is unexpectedly high for an extracellular volume fraction. It is possible that our assumed arterial input function has under-estimated arterial Gd-DTPA concentrations and therefore over-estimated K^{trans} and ν_e (see below). However, if ν_e is considered as a pharmacokinetic parameter then the upper limit of its value ($\nu_e < 1$) may not strictly apply.

How should we interpret the fall in ν_e following CA-4-P treatment? An increase in vascular permeability to macromolecules may occur as a result of CA-4-P administration[16] and this would lead to oedema and an increase in extracellular space. This is certainly suggested by the increase in T_1 shown at 24 h following 100 mg kg^{-1} CA-4-P (Fig. 3). Later consequences of the anti-vascular effects include cell death and therefore an increase in necrotic fraction and extracellular space. These effects are not consistent with a fall in ν_e. However, CA-4-P results in the complete shutdown of a large proportion of tumour blood vessels[3] such that some parts of the tumour are no longer in rapid contact with flowing blood plasma (compared to the 5 min total time duration of our kinetic measurements). This would explain the fall in ν_e. Note that this 'apparent ν_e' is now the sub-set of the extravascular extracellular space to which Gd-DTPA still has access through perfusion and diffusion.

The relationship between K^{trans} and physiological parameters has been described as follows.[13] Under flow-limited conditions K^{trans} equals the blood plasma flow per unit volume of tissue; under permeability-limited conditions K^{trans} equals the permeability surface area product per unit volume of tissue. Van der Sanden *et al.*[19] found a positive correlation between Gd-DTPA uptake rates in the 9L glioma (implanted in rat brains) and the perfused microvessel density or surface area. They concluded that, in this case, blood flow rate far exceeded tracer transport across the microvascular endothelium. Although the 9L tumour was found to be in permeability-limited conditions ($K^{trans} = P \cdot S$), they also noted that Gd-uptake measurements may be of value in evaluating therapies that affect the perfused microvessel density or surface area, such as anti-angiogenic therapy. We note an apparent paradox here. Even in the situation where $K^{trans} = P \cdot S$, changes in K^{trans} may still be useful for quantifying anti-angiogenic (or anti-vascular) treatments. One interpretation is that it is the vascular surface-area term, which will be most sensitive to such treatments. Indeed, the permeability to macromolecules may actually be increased under these circumstances. The effects of anti-vascular drugs on the permeability of vessels in extra-cranial tumours are uncertain. The close relationship between K^{trans} and IAP-derived tumour blood flow rate values in P22 tumours before and after combretastatin treatment suggests that flow-limited conditions exist for Gd-DTPA kinetics such that K^{trans} may provide a good estimate for blood flow rate in this tumour model.

Image segmentation

The results obtained from data averaged according to the image segmentation protocol were very similar to those obtained when data were averaged over the entire tumour. The image segmentation approach has the advantage that spatial information is retained. However, when data were analysed on a pixel-by-pixel basis, the response to CA-4-P appeared to be different in some ways, in particular with an increase in k_{ep}. We interpret these k_{ep} changes as an artefact of fitting noisy data and the very wide range of values that were accepted, e.g. addition of noise to exponential data may lead to a larger error and larger positive bias in the estimated rate constant (k_{ep}) than in the scaling term, K^{trans}. The individual pixel data has relatively low signal:noise in

untreated tumours (it corresponds to pixel dimensions of 0.12×0.12 mm) and the signal:noise is lower still in treated tumours. The image segmentation approach has the advantage over pixel-by-pixel analysis of a greater signal:noise and more reliable fitting of data. It also has an advantage compared to averaging data over the whole tumour in that that spatial information is retained. In general, fitting a single exponential term to a sum of exponentials, such as would result from averaging of heterogeneous pixels, can be problematic. To some extent this problem is minimized using the segmentation method, since groups of pixels having similar kinetic patterns are identified. It is not entirely eliminated as a maximum of eight different patterns is used.

Analysis of Gd-DTPA kinetic parameters according to the distance from the tumour edge did not, in general, show any substantial differences between the response to CA-4-P between rim, intermediate and central tumour regions. The only exception to this was for the group of animals examined 6 h after 10 mg kg^{-1} CA-4-P, in which the Gd-DTPA AUC value was significantly higher in the rim than in the tumour centre. This is in contrast to the results of previous IAP uptake studies in this tumour model which do show a bigger relative effect in the tumour centre than in the periphery.[4] Several factors may have contributed to a general failure to detect spatial differences in the response to CA-4-P: (i) the untreated tumours had a relatively uniform pattern of tumour blood flow; (ii) the image segmentation method may have reduced the effective spatial resolution to an excessive extent; (iii) the tumour edge was not always easily defined. Although the averaging resulting from image segmentation is inevitably a compromise between pixel-by-pixel analysis (where low signal:noise restricts model fitting) and whole tumour analysis, the segmentation procedure should be able to identify rapid Gd-DTPA kinetics at the rim and slow kinetics in the centre, if these features are consistently present. Calculation of the Gd-DTPA AUC (which shows a similar dose- and time-dependant pattern of CA-4-P effects to K^{trans}) on a pixel-by-pixel basis was more robust than for the other parameters since this involves a simple summation rather than model fitting. Even with the maximal spatial resolution given by this analysis, there was only a limited indication of spatial dependency.

Arterial input function

In order to obtain absolute measurements of tumour blood flow it is necessary to include information about the arterial concentration of the tracer during the tissue uptake period. This has been done by arterial sampling in the case of radioactively labelled IAP. Although it is possible to obtain arterial Gd-DTPA concentrations either by arterial sampling[20] or MRI measurements in large vessels,[21] these approaches are not straightforward. A very detailed study in anaesthetised rats with various doses of ^{153}Gd-DTPA (and ^{99m}Tc-DTPA) found that the plasma and urine data gave a best fit to a three compartment open model corresponding to a three-exponential fit.[14] This study additionally showed that there were no differences in plasma pharmacokinetic parameters between doses of 0.01, 0.1 and 1.0 mmol kg^{-1}, nor between the gadolinium and technetium chelates. The use of a two exponential version of Wedeking's results for modelling MRI data has been reported.[21,22] We have used the model rate constants and apparent volume of distribution presented by Wedeking *et al.*[14] for 0.1 mmol kg^{-1} Gd-DTPA to calculate parameters for a three-exponential function. These exponential rate constants are very similar to those calculated from MRI measurements in the rat inferior vena cava[23] (i.e. $\alpha_1 = 1.073$ min^{-1}, $\alpha_2 = 0.152$ min^{-1} and $\alpha_3 = 0.018$ min^{-1}) while the fastest and slowest rate constants correspond closely to the parameters of a two-exponential fit determined by arterial sampling following ^{99m}Tc-DTPA injection.[24] The duration of the bolus injection (5 s) is relatively short compared to the imaging time-resolution (11.8 s). This finite bolus and the subsequent mixing in the plasma may have some effect on fitted parameters. However we have not modified the description of Gd-DTPA pharmacokinetics modelled by Wedeking *et al.*,[14] who used a bolus injection of similar, if slightly longer, duration (10–15 s).

We have firstly assumed that Wedeking *et al.*'s model parameters are appropriate for untreated, anaesthetized rats. We note that two features of any assumed or estimated arterial input function will affect the fitted parameters in different ways. The shape of the arterial input function will be particularly important in estimating the exponential rate constant, k_{ep}, whereas K^{trans} will depend on an accurate estimate of the amplitude of the arterial input function. Some studies[22] do not derive K^{trans} explicitly, but also include the arterial input function scaling in the fitted parameter. However, it is not possible to obtain ν_e without knowing the amplitude of the arterial input function. On the other hand, errors in arterial input function scaling will lead to incorrect values of ν_e as well as K^{trans}. Rozijn *et al.*[22] also investigated the effect of describing the initial mixing in plasma by a gamma variate function, i.e. not assuming that Gd-DTPA mixes instantaneously in plasma. They found that inclusion of the gamma function had an adverse effect on fitting tumour data but that the first few tumour measurements should be discarded (until peak plasma concentration was reached). Although initial data points have not been discarded in the current study, the time of peak plasma concentration of about 12 s[22] corresponds to just one data point given the limited time resolution we have used.

A second assumption is that these parameters are also appropriate for rats treated with combretastatin. Given that CA-4-P has been shown[4] to have significant cardiovascular effects (e.g. 30% increase in mean arterial

blood pressure 1 h after 100 mg kg^{-1}) especially within the first few hours of treatment, we need to be very cautious about the reliability of this assumed arterial input function, in particular for the measurements made after 1 h. The use of population-derived arterial input functions allows estimation of standard parameters describing Gd-DTPA kinetics (e.g. K^{trans} and ν_e) and avoids the technical difficulties and possible errors associated with measuring arterial input functions from large blood vessels in MR images (e.g. due to combined T_1 and T_2 relaxation effects and to time-resolution and signal:noise limitations). However, accurate measurement of Gd-DTPA arterial concentrations is desirable, especially in evaluating drugs with systemic cardiovascular effects. The effect of CA-4-P on rat Gd-DTPA plasma kinetics and the consequences for K^{trans} and k_{ep} estimation have not yet been determined.

To summarize the main results of this study: (i) The area under the Gd-DTPA concentration–time curve from 0–94 s (AUC) and the model parameter K^{trans} both gave significantly smaller values in P22 tumours treated with CA-4-P (10 or 100 mg kg^{-1}) than in untreated tumours; (ii) these effects were both time- and dose-dependant; (iii) K^{trans} was similar in magnitude to tumour blood flow determined by IAP uptake in both untreated and treated tumours; (iv) a clear difference in the effects of CA-4-P between the rim and the centre of the tumour was not demonstrated.

CONCLUSIONS

DCE-MRI with Gd-DTPA can be used routinely in clinical practice to provide information about tumour vasculature.[7] However, the parameters that can be derived from Gd-DTPA kinetics do not give an unambiguous measurement of tumour physiological parameters, particularly blood flow. In this study, DCE-MRI was used to obtain the model parameters K^{trans}, k_{ep} and ν_e in tumours in untreated rats and in animals treated with CA-4-P with an experimental protocol similar to that used in patients during phase I clinical trials of this drug.[6] The changes in K^{trans} were reflective of changes in blood flow rate determined in parallel groups of animals from the uptake of ^{125}I-IAP, although the magnitude of changes in K^{trans} was smaller than the blood flow changes. It is not clear whether blood flow contributes directly to K^{trans} in this situation or whether K^{trans} is determined by the surface area of (open) blood vessels and hence $P{\cdot}S$, the permeability–surface area product. In any case, these results suggest that K^{trans} values for Gd-DTPA uptake into tumours could be a useful non-invasive indicator of blood flow changes induced by anti-vascular agents such as combretastatin.

REFERENCES

1. Folkman J. Addressing tumor blood vessels. *Nat. Biotechnol.* 1997; **15**: 510.
2. Chaplin DJ, Dougherty GJ. Tumour vasculature as a target for cancer therapy. *Br. J. Cancer* 1999; **80**(Suppl 1), 57–64.
3. Dark GG, Hill SA, Prise VE, Tozer GM, Pettit GR, Chaplin DJ. Combretastatin A-4, an agent that displays potent and selective toxicity toward tumor vasculature. *Cancer Res.* 1997; **57**: 1829–1834.
4. Tozer GM, Prise VE, Wilson J, Locke RJ, Vojnovic B, Stratford MR, Dennis MF, Chaplin DJ. Combretastatin A-4 phosphate as a tumor vascular-targeting agent: early effects in tumors and normal tissues. *Cancer Res.* 1999; **59**: 1626–1634.
5. Grosios K, Holwell SE, McGown AT, Pettit GR, Bibby MC. In vivo and in vitro evaluation of combretastatin A-4 and its sodium phosphate prodrug. *Br. J. Cancer* 1999; **81**: 1318–1327.
6. Galbraith SM, Taylor NJ, Maxwell RJ, Lodge M, Tozer GM, Baddeley H. Combretastatin A4 phosphate (CA4P) targets vasculature in animal and human tumours. *Br. J. Cancer* 2000; **83**(Suppl 1), 12.
7. Taylor JS, Tofts PS, Port R, Evelhoch JL, Knopp M, Reddick WE, Runge VM, Mayr N. MR imaging of tumor microcirculation: promise for the new millennium. *J. Magn. Reson. Imag.* 1999; **10**: 903–907.
8. Maxwell RJ, Wilson J, Tozer GM, Barber PR, Vojnovic B. Segmentation of magnetic resonance images according to contrast agent uptake kinetics using a competitive neural network. In Artificial Neural Networks in Medicine and Biology, Malmgren H, Borga M, Niklasson L (eds). Springer: London, 2000; 93–98.
9. Tozer GM and Shaffi KM. Modification of tumour blood flow using the hypertensive agent, angiotensin II. *Br. J. Cancer* 1993; **67**: 981–988.
10. Kety S. Blood-tissue exchange methods. Theory of blood-tissue exchange and its application to measurement of blood flow. *Meth. Med. Res.* 1960; **8**: 223–227.
11. Tozer GM, Morris CC. Blood flow and blood volume in a transplanted rat fibrosarcoma: comparison with various normal tissues. *Radiother. Oncol.* 1990; **17**: 153–165.
12. Tozer GM, Shaffi KM, Prise VE, Cunningham VJ. Characterisation of tumour blood flow using a 'tissue-isolated' preparation. *Br. J. Cancer* 1994; **70**: 1040–1046.
13. Tofts PS, Brix G, Buckley DL, Evelhoch JL, Henderson E, Knopp MV, Larsson HB, Lee TY, Mayr NA, Parker GJ, Port RE, Taylor J, Weisskoff RM. Estimating kinetic parameters from dynamic contrast-enhanced T(1)-weighted MRI of a diffusable tracer: standardized quantities and symbols. *J. Magn. Reson. Imag.* 1999; **10**: 223–232.
14. Wedeking P, Eaton S, Covell DG, Nair S, Tweedle MF, Eckelman WC. Pharmacokinetic analysis of blood distribution of intravenously administered 153Gd-labeled Gd(DTPA)2- and 99mTc (DTPA) in rats. *Magn. Reson. Imag.* 1990; **8**: 567–575.
15. Gibaldi M, Perrier D. Pharmacokinetics. Marcel Dekker: New York, 1982.
16. Kanthou C, Prise VE, Wilson J, Tozer GM. Proceedings of the AACR Annual meeting 2001.
17. Beauregard DA, Thelwall PE, Chaplin DJ, Hill SA, Adams GE, Brindle KM. Magnetic resonance imaging and spectroscopy of combretastatin A4 prodrug-induced disruption of tumour perfusion and energetic status. *Br. J. Cancer* 1998; **77**: 1761–1767.
18. Maxwell RJ, Nielsen FU, Breidahl T, Stødkilde-Jørgensen H, Horsman MR. Effects of combretastatin on murine tumours monitored by 31P MRS, 1H MRS and 1H MRI. *Int. J. Radiat. Oncol. Biol. Phys.* 1998; **42**: 891–894.
19. van der Sanden BP, Rozijn TH, Rijken PF, Peters HP, Heerschap A, van der Kogel AJ, Bovee WM. Noninvasive assessment of the functional neovasculature in 9L-glioma growing in rat brain by dynamic 1H magnetic resonance imaging of gadolinium uptake. *J. Cereb. Blood Flow Metab.* 2000; **20**: 861–870.
20. Larsson HB, Stubgaard M, Frederiksen JL, Jensen M, Henriksen O, Paulson OB. Quantitation of blood-brain barrier defect by magnetic resonance imaging and gadolinium-DTPA in patients with multiple sclerosis and brain tumors. *Magn. Reson. Med.* 1990; **16**: 117–131.
21. Su MY, Jao JC, Nalcioglu O. Measurement of vascular volume

fraction and blood-tissue permeability with a pharmacokinetic model: studies in rat muscle tumors with dynamic Gd-DTPA enhanced MRI. *Magn. Reson. Med.* 1994; **32**: 714–724.
22. Rozijn TH, van der Sanden BPJ, Heerschap A, Creyghton JHN, Bovee WMMJ. Influence of the pharmacokinetic model on the quantification of the Gd-DTPA uptake rate in brain tumours using direct T_1 measurements. *MAGMA* 1998; **6**: 37–43.
23. Daldrup HE, Shames DM, Husseini W, Wendland MF, Okuhata Y, Brasch RC. Quantification of the extraction fraction for gadopentetate across breast cancer capillaries. *Magn. Reson. Med.* 1998; **40**: 537–543.
24. Pedersen M, Morkenborg J, Jensen FT, Stodkilde-Jorgensen H, Djurhuus JC, Frokioer J. In vivo measurements of relaxivities in the rat kidney cortex. *J. Magn. Reson. Imag.* 2000; **12**: 289–296.

